DOI: 10.1002/cmdc.201300297

Histone Deacetylase Inhibitors with Enhanced Enzymatic Inhibition Effects and Potent in vitro and in vivo Antitumor Activities

Lei Zhang,*[a] Yingjie Zhang,[b] C. James Chou,[c] Elizabeth S. Inks,[c] Xuejian Wang,[d] Xiaoguang Li,[b] Jinning Hou,[b] and Wenfang Xu*[b]

In the present work, a series of small molecules were designed and synthesized based on structural optimization. A significant improvement in the enzyme inhibitory activity of these compounds was discovered. Moreover, the tested compounds have moderate preference for class I HDACs over HDAC6, as demonstrated by enzyme selectivity assays. In vitro antiproliferation assay results show that representative compounds can selectively inhibit the growth of non-solid lymphoma and leukemic cells such as U937, K562, and HL60. In the in vivo antitumor assay, (*S*)-4-(2-(5-(dimethylamino)naphthalene-1-sulfonamido)-2-phenylacetamido)-*N*-hydroxybenzamide (**D17**) showed better performance than SAHA in blocking U937 tumor growth. Western blot analysis revealed that representative molecules can block the function of both class I HDACs and HDAC6. More importantly, our western blot results reveal that the levels of some oncogenic proteins (p-Akt in the PI3K/AKT/mTOR signal pathway, c-Raf and p-Erk in the MAPK signal pathway) were dramatically down-regulated by our compounds in the U937 cell line rather than MDA-MB-231 cells. This distinction in cellular mechanism might be an important reason why the U937 cell line was found to more sensitive to our HDAC inhibitors than the MDA-MB-231 cell line.

Introduction

Histone deacetylases (HDACs) are a class of enzymes responsible for removing acetyl groups from the ε-*N*-acetyl group of histone lysine residues. To date, 18 HDACs have been discovered, and they are divided into four classes.[1] Class I HDACs include HDAC 1, 2, 3 and 8; within this class, HDAC 1, 2 and 8 are primarily found in the nucleus, while HDAC 3 is found in both the nucleus and cytoplasm. Class II HDACs (IIa: HDAC 4, 5, 7 and 9; IIb: HDAC 6 and 10) are able to shuttle in and out of the nucleus. Members of classes I and II are also called "classical zinc-dependent" HDACs. Class III HDACs (known as sirtuins, Sirt1–7) are a set of NAD-dependent enzymes. The class IV HDAC (HDAC 11) also exists in both the nucleus and cytoplasm but is considered as an atypical isoform and thus placed in a category of its own based on low sequence similarity to the others.

Acetylation and deacetylation of histones and non-histone proteins by histone acetylases (HATs) and HDACs play important roles in the regulation of gene expression and transcription.[2] The effects include signal transduction, protein phosphorylation, cell-cycle regulation, proliferation, apoptosis, cardiac development, and so on.[3] Overexpression and aberrant recruitment of HDACs have significant roles in tumorigenesis.[4]

Histone deacetylase inhibitors (HDACIs) have been proven to alter gene expression by blocking the action of HDACs and inducing hyperacetylation of histones.[5] A number of structurally diverse HDACIs have shown potent antitumor efficacy in various stages of clinical trials. Suberoyl anilide hydroxamic acid (SAHA)[6] and FK228[7] have been approved by the US Food and Drug Administration (FDA) for the treatment of advanced cutaneous T-cell lymphoma (CTCL).

In order to develop novel HDACIs as antitumor agents, a series of small molecules was designed and synthesized based on virtual screening results.[8] A phenylglycine-containing structure (**4h**) was discovered to have good performance in the enzyme inhibition and tumor cell growth inhibition assays. Structural modifications were performed in the present work in discovery of more potent molecules (Scheme 1). To improve the activities of synthesized compounds, aromatic groups introduced to substitute with the *tert*-butyloxycarbonyl (BOC) group of **4h** were designed to interact with hydropho-

[a] *Dr. L. Zhang*
Department of Pharmacy, School of Medicine, Qingdao University
308 Dengzhou Road, Qingdao, Shandong 266071 (China)
E-mail: lei@qdu.edu.cn

[b] *Dr. Y. Zhang, X. Li, J. Hou, Prof. W. Xu*
Department of Medicinal Chemistry
School of Pharmacy, Shandong University
44 Wenhua Xi Road, Jinan, Shandong 250012 (China)
E-mail: xuwenf@sdu.edu.cn

[c] *Prof. C. J. Chou, Dr. E. S. Inks*
Department of Drug Discovery & Biomedical Sciences
South Carolina College of Pharmacy, Medical University of South Carolina
280 Calhoun Street, MSC 141, Charleston, SC 29425 (USA)

[d] *Dr. X. Wang*
School of Pharmacy & Biology Science, Weifang Medicinal University
288 Shengli E Street, Kuiwen, Weifang, Shandong 261042 (China)

Supporting information for this article is available on the WWW under http://dx.doi.org/10.1002/cmdc.201300297.

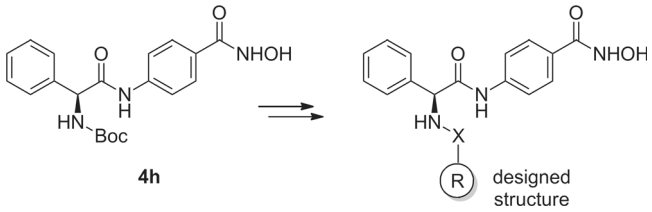

Scheme 1. Design of new molecules based on the structure of **4h**. X group is CO, SO_2 or CONH; R group is substituted aromatic rings.

bic residues (Phe 155, Phe 210 and Tyr 308) in the active site of HDAC2 (Figure 1).

Results and Discussion

Chemistry

Based on lead structure **4h**, a series of phenylglycine-containing hydroximic acid derivatives were synthesized according to the procedures described in Scheme 2. The starting material (*S*)-2-amino-2-phenylacetic acid was protected by a Boc group; the other material, 4-aminobenzoic acid, was protected by a methyl ester. Intermediate (*S*)-methyl 4-(2-((*tert*-butoxycarbonyl)amino)-2-phenylacetamido)benzoate (**a**) was derived by coupling these two products. Subsequent N-deprotection of intermediate **a** and condensation with various acyl chlorides, sulfonyl chlorides, and aryl amines afforded **c1**–**c19**. Target compounds **D1**–**D19** were derived by treating the corresponding intermediates (**c1**–**c19**) with potassium hydroxylamine in methanol.

Biological evaluation

An enzymatic inhibition assay was performed using HeLa cell nucleus extract containing a mixture of HDAC isoforms. Compared with **4h**, significant improvements in inhibitory activities of the derived molecules were observed, indicating that aromatic R groups enhance the inhibitor–receptor interactions by binding to hydrophobic residues (Phe 155, Phe 210 and Tyr 308; Table 1). Carbamido-group-containing molecule **D18** performed the best in the enzymatic inhibition assay, exhibiting an IC_{50} value of 7.5 nM. Molecules with larger aromatic groups (e.g., naphthalene ring) have potent inhibitory activities: **D3** (14.3 nM), **D5** (15.6 nM), **D16** (23.5 nM) and **D17** (9.7 nM). Chlorine substitution of the phenyl ring apparently decreases the activity as compared with **D7**, such as **D1** (348 nM), **D2** (95.5 nM) and **D10** (125 nM). However, bromine substitution of the phenyl group improves the activity (**D13**: 13.0 nM). Hydrophobic groups such as *tert*-butyl and strongly electrophilic groups such as trifluoromethyl have a negative effect on the inhibitory activity (**D6**: 105 nM, **D8**: 85.5 nM; **D18**: 7.5 nM, **D19**: 47.7 nM). With respect to fluorine and methoxy substituents, the *para* position gives rise to more potent derivatives than the *ortho* position (**D4** vs. **D9**; **D11** vs. **D12**), although the difference is not significant. The position of substitution also plays an important role in the activity of naphthalene-sulfonyl-containing derivatives; compounds substituted at the 1-position (**D5**) are more potent than those substituted at the 2-position (**D16**). Furthermore, a polar group on the naphthalene ring improves the enzymatic inhibitory activity of the derivative (**D17**). From the above findings, we conclude that larger aromatic R groups are beneficial to the HDAC inhibitory activity of the compounds. In terms of the substituents on the aromatic ring, polar groups (not strong electrophilic groups) are favored, and the positions of the substituent groups also affect the activity.

To characterize the isoform selectivity of these molecules, representative compounds **D3**, **D5**, **D13**, **D17** and **D18** were tested against HDAC1, HDAC2, HDAC3 and HDAC6 (Table 2). The result show that these four molecules display preference for HDAC1, HDAC2 and HDAC3 over HDAC6. As to class I HDACs, the tested molecules show modest selectivity for HDAC1 and HDAC3 over HDAC2. **D18** exhibits the most potent activity in the selectivity assay, with IC_{50} values of 4.8 nM,

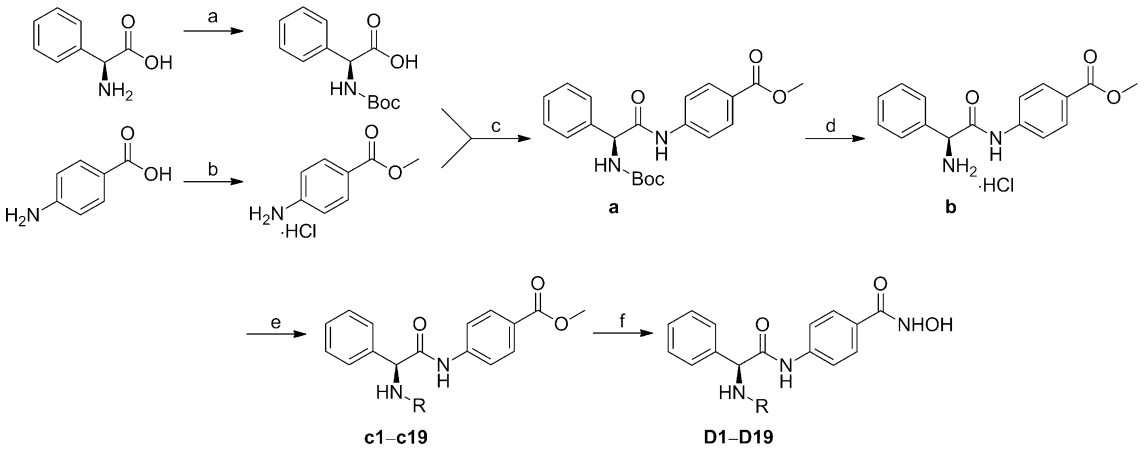

Scheme 2. Synthesis of compounds **D1**–**D19**. *Reagents and conditions*: a) $(Boc)_2O$, Et_3N, $MeOH/H_2O$ (3:1), 8 h, 25 °C, 86%; b) CH_3COCl, CH_3OH, 5 h, 75 °C, 77%; c) TBTU, Et_3N, THF, 8 h, 25 °C, 75%; d) EtOAc, HCl, 5 h, 25 °C, 68%; e) RSO_2Cl, RCOCl, $NaHCO_3$, THF/H_2O, RT, 8 h, 70–82%; 1) RNH_2, triphosgene, dioxane, 110 °C, 8 h; 2) Et_3N, CH_2Cl_2, RT, 5 h, 43–45% (two steps); f) NH_2OK, MeOH, RT, 2 h, 33–54%.

Table 1. Enzyme inhibitory activities of the derived molecules determined using HeLa cell nucleus extract containing a mixture of HDAC isoforms.

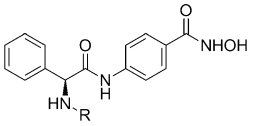

Compd	R	IC_{50} [nM][a]
D1	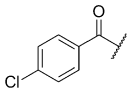	348.6 ± 21.2
D2		95.5 ± 4.6
D3	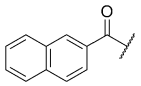	14.3 ± 0.9
D4	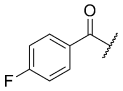	25.5 ± 1.6
D5	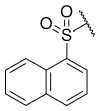	15.6 ± 1.1
D6	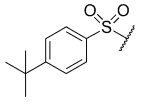	105.5 ± 9.7
D7		28.7 ± 2.2
D8	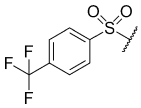	85.5 ± 6.7
D9		60.2 ± 4.7
D10	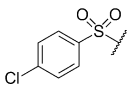	125.5 ± 10.6
D11	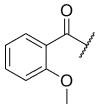	33.6 ± 2.3
D12	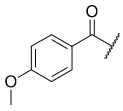	20.5 ± 1.1
D13	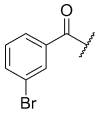	13.7 ± 0.7
D14	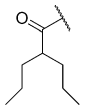	22.8 ± 1.8
D15	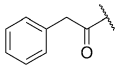	34.6 ± 2.4
D16	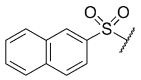	23.5 ± 1.7

Table 1. (Continued)

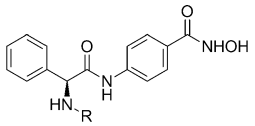

Compd	R	IC_{50} [nM][a]
D17	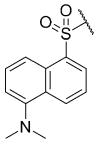	9.7 ± 0.3
D18	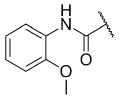	7.5 ± 0.2
D19	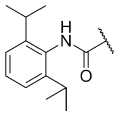	47.7 ± 3.3
4h		144.4 ± 9.7
SAHA		145.6 ± 7.6

[a] Values represent the mean ± SD of three independent experiments performed in triplicate.

Table 2. HDAC isoform selectivity of representative compounds.[a]

Compd	IC_{50} [nM]			
	HDAC1	HDAC2	HDAC3	HDAC6
D3	28.7 ± 1.9	243.5 ± 11.7	16.8 ± 1.2	375.8 ± 19.7
D5	30.7 ± 1.3	170.6 ± 9.7	23.1 ± 1.1	294.5 ± 11.7
D13	11.8 ± 0.9	89.2 ± 4.7	8.5 ± 0.3	195.8 ± 11.9
D17	24.7 ± 1.4	106.7 ± 8.9	24.4 ± 1.5	365.9 ± 20.6
D18	4.8 ± 0.3	19.5 ± 1.4	5.9 ± 0.4	294.2 ± 22.3
SAHA	76.1 ± 2.6	256.3 ± 11.4	28.1 ± 1.8	118.2 ± 10.8

[a] Values represent the mean ± SD of three independent experiments performed in triplicate.

19.5 nM, 5.9 nM and 294.2 nM against HDAC1, HDAC2, HDAC3 and HDAC6, respectively.

Modeling

Docking was performed to predict the binding patterns of the derived molecules in the active site of HDAC2 (Figure 1). There is a narrow tunnel in the active site of HDAC2, and the zinc ion is located at the end of the tunnel. An open pocket that is surrounded by hydrophobic residues (Phe 155, Phe 210 and Tyr 308) lies under the opening of the gap (Figure 1 a). **D5** (Figure 1 b) and **D17** (Figure 1 d) are predicted to have similar binding patterns in the active site of HDAC2. The hydroximic acid group chelates to the zinc ion giving rise to the tight binding to the receptor. The linker locating in the tunnel is predicted to participate in strong hydrophobic interactions

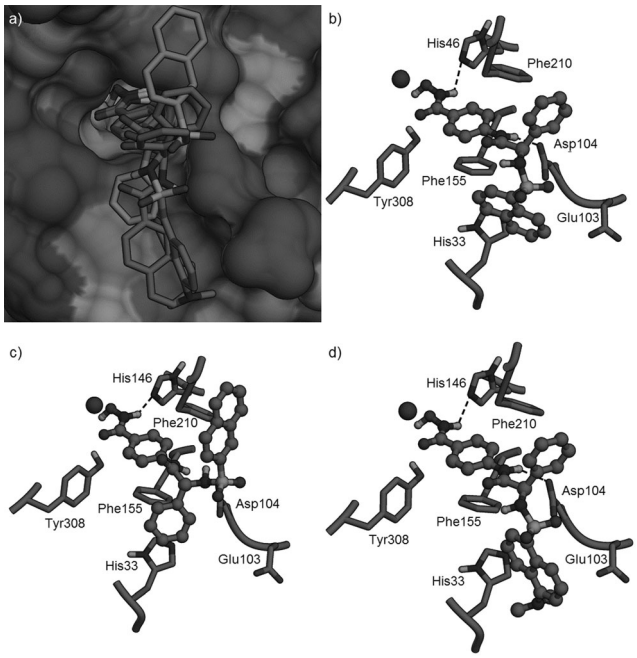

Figure 1. a) Predicted binding of **D5**, **D16** and **D17** to HDAC2 in surface representation; the binding pattern of b) **D5**, c) **D16** and d) **D17** in the active site of HDAC2.

with residues around the gap. The benzene ring of the phenylglycine group is predicted to interact with the hydrophobic area of the opening, further contributing to the binding. According to our modeling results, the external motif binding to the pocket under the opening has good spatial matching with the surface of the active site. All these effects in combination enhance the ligand–receptor interactions. However, according to our predictions, **D16** has a different binding mode (Figure 1c); in our model, both the phenyl ring and the naphthalene ring in the external motif locate in the opening of the gap. The hydrogen-bonding interactions predicted to form between the ligand and the active site of HDAC2 are also likely to play a significant role in binding. According to the docking results, the NH group of the hydroximic acid moiety of all these molecules is involved in hydrogen-bonding interaction with NE2 of His146. In addition, another key residue for hydrogen bonding, Asp104, is also predicted to interact through a hydrogen bond with NH1 of **D5** and NH1 of **D17**. In contrast, the docking with **D16** shows has no hydrogen-bonding interactions with Asp104. This predicted lack of interaction with the pocket through hydrogen bonding is presumed to be the reason for the comparatively weak activity of **D16** in the enzyme inhibition assay.

To evaluate the antiproliferation activity of the synthesized molecules, MTT assays were performed using U937, K562, HL60, MCF7 PC3 and MDA-MB-231 cell lines. The derived compounds were firstly screened against U937 cells at 2 μM. Molecules exhibiting >50% inhibition were then selected for further evaluation in antiproliferation assays against the broader panel, and their IC_{50} values were calculated (Table 3). On the whole, lymphoma and leukemic cell lines (U937, K562, and HL60) are more sensitive to these molecules than the solid tumor cell lines (MCF7, PC3, and MDA-MB-231); this is in line with published preclinical and clinical research results, which indicate that the therapeutic efficacy of HDACIs is restricted predominantly to hematological malignancies.[9] Compounds **D3** (1.32 μM) and **D17** (1.24 μM) have lower IC_{50} values than SAHA in inhibiting the growth of U937 cells. As for K562 cells, most of the derived compounds (except **D11** and **D12**) show better performance than SAHA, and **D17** is the most active molecule (IC_{50} = 0.70 μM). Only **D11** has a better IC_{50} value than SAHA in blocking HL60 cell growth (**D11**: 0.78; SAHA: 1.44). Compounds **D3** (2.92 μM) and **D4** (2.04 μM) outperform SAHA (5.09 μM) in the MCF7 cell growth inhibition assays. Only three compounds have larger IC_{50} values than SAHA in the PC3 cell assays, of which **D18** (IC_{50} = 1.51 μM) is the most active. **D3** (IC_{50} = 4.23 μM) demonstrated the best performance in inhibiting the growth of MDA-MB-321 cells.

The human leukemic monocyte lymphoma cell line U937 was the most sensitive to the tested molecules (mean IC_{50} value of 1.51 μM). Therefore, the U937 cell line was selected for in vivo antitumor assays. The most effective U937 cell growth inhibitor, **D17**, which also has the highest water solubility, was selected for the in vivo antiproliferation assays. As a preliminary

Table 3. Tumor cell growth inhibitory activities of synthesized compounds against a panel of cancer cell lines.[a]

Compd	IC_{50} [μM]					
	U937	K562	HL60	MCF7	PC3	MDA-MB-231
D3	1.32 ± 0.07	1.19 ± 0.04	3.15 ± 0.13	2.92 ± 0.15	3.77 ± 0.27	4.23 ± 0.33
D4	1.64 ± 0.08	1.59 ± 0.06	4.55 ± 0.21	2.04 ± 0.17	5.88 ± 0.36	4.78 ± 0.44
D5	1.63 ± 0.09	0.93 ± 0.02	2.88 ± 0.16	8.66 ± 0.73	10.1 ± 0.57	5.12 ± 0.34
D7	1.77 ± 0.06	1.47 ± 0.07	2.02 ± 0.15	10.8 ± 0.93	5.67 ± 0.35	6.22 ± 0.24
D11	1.71 ± 0.03	3.16 ± 0.11	0.78 ± 0.02	8.23 ± 0.32	20.5 ± 1.73	6.67 ± 0.25
D12	1.55 ± 0.04	1.93 ± 0.12	1.80 ± 0.09	6.28 ± 0.33	3.00 ± 0.15	4.65 ± 0.24
D13	1.39 ± 0.03	1.58 ± 0.06	1.53 ± 0.04	9.71 ± 0.44	31.6 ± 2.33	4.47 ± 0.31
D17	1.24 ± 0.02	0.70 ± 0.01	3.66 ± 0.13	5.34 ± 0.22	3.31 ± 0.16	4.46 ± 0.28
D18	1.31 ± 0.07	1.55 ± 0.05	3.83 ± 0.29	5.14 ± 0.43	1.51 ± 0.05	4.34 ± 0.26
Av.[b]	1.51 ± 0.05	1.57 ± 0.06	2.69 ± 0.14	6.57 ± 0.41	9.48 ± 0.66	4.99 ± 0.30
SAHA	1.38 ± 0.09	1.86 ± 0.07	1.44 ± 0.06	5.09 ± 0.21	6.33 ± 0.22	4.70 ± 0.35

[a] Values represent the mean ± SD of three independent experiments performed in triplicate. [b] The mean (Av.) IC_{50} value of the test compounds against each cell line.

investigation of the in vivo antiproliferative activity of **D17**, only one concentration (100 mg kg^{-1} d^{-1}) was applied, and SAHA was used as a positive control. After 16 days of intragastric administration, the mice were euthanized, and tumor weights were measured. The mean weight of tumors in the negative control group was found to be 2.66 g (SD: 37%); the analogous values for SAHA- and **D17**-treated groups were 2.00 g (SD: 26%) and 1.24 g (SD: 18%), respectively (Figure 2a). The inhibitory ratio of compound **D17** is 53.57%, compared with SAHA with a value of 24.97% (Figure 2b). The results show that **D17** exhibits improved antitumor activity over SAHA. Tumor volumes were measured every two days, and the results correlate with tumor weights (Figure 2c and Figure 3). All these results confirm with statistical significance that compound **D17** has greater in vivo potency than SAHA. Compound **D17** is safe, as evidenced by the fact that no loss in body weight was observed (measured every two days; Figure 2d). Moreover, no clear signs of toxicity in liver and spleen were detected.

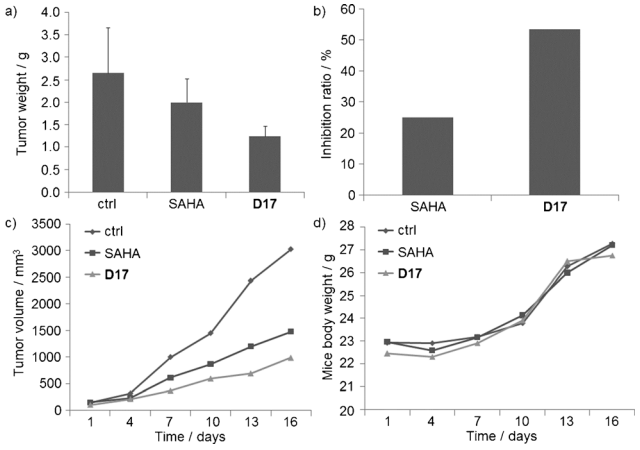

Figure 2. Results of in vivo evaluation of **D17**. The negative control (vehicle only) and positive control (SAHA) groups are included for reference. a) Tumor weight plot; b) inhibitory ratio plot; c) tumor volume plot; d) mice body weight plot.

Western blot studies were performed to evaluate the intracellular functions of representative compounds (Figure 4). The results show that these investigated molecules (**D3**, **D5**, **D13**, **D17**, and **D18**) are cell permeable and can inhibit intracellular and even nuclear HDACs, as determined by monitoring the acetylation levels of tubulin (target of HDAC6), histones H3 and H4 (targets of HDAC1 and HDAC2), and p21, which is substrate of class I HDACs. All the compounds tested increase the acetylation levels of tubulin under 6 h treatment, indicating that the tested molecule can efficiently block the function of HDAC6 in U937 cells. After 24 h, the effect of **D3**, **D5**, and **D13** on the increase in acetylated tubulin levels is still significant, but the action of **D17** and **D18** are decreased. At both time points, all the tested compounds show a higher capacity than SAHA in increasing the levels of the cyclin-dependent kinase (CDK) inhibitor p21. This indicates that the representative compounds are effective and stable class I HDAC inhibitors. The tested molecules are more effective at inducing the acetylation levels of histone H3 than those of histone H4, which correlates with the enzyme selectivity assay results.

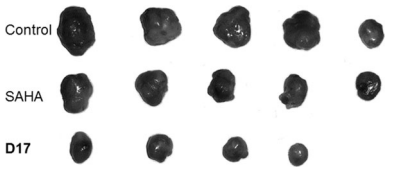

Figure 3. Dissected tumor tissues taken from mice after intragastric administration of 100 mg kg^{-1} d^{-1} of **D17** or SAHA as a positive control. All the tumors were dissected at the 16th day of administration.

HDAC inhibitors are limited by low and ineffective concentrations in solid tumors.[9] The FDA-approved drugs SAHA and FK228 have no clear efficacy in treating relapsed or refractory breast, colorectal, non-small-cell lung, or metastatic head and neck cancers, for example, as proven by various clinical trials.[10] To explore the reason why hematological tumor cell lines are more sensitive to HDACIs than solid tumor cell lines, we performed a series of western blot analyses to investigate the various effects of compounds **D3** and **D17** on the signaling cascades between non-solid (U937) and solid (MDA-MB-231) tumor cell lines (Figure 5). The c-Raf and Erk proteins are two crucial kinases in activating the MAPK pathway. Phosphorylated Erk (p-Erk) is the active form of this protein. MDA-MB-231 cells have an overactive MAPK pathway, and the selected mol-

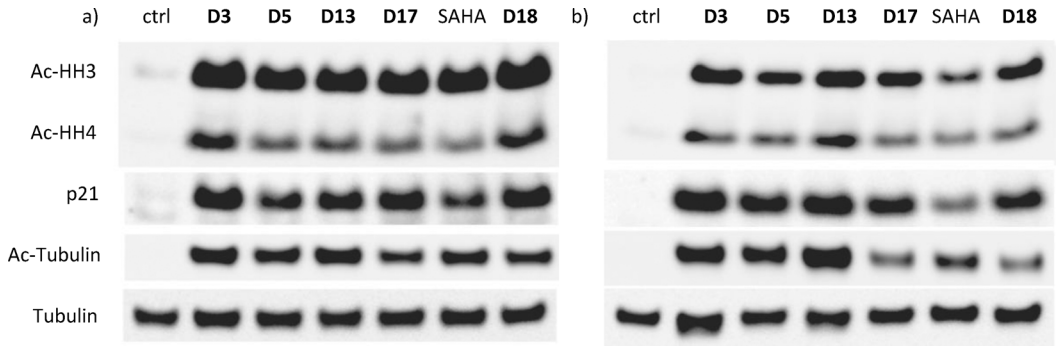

Figure 4. Western blot analysis of acetylated histone H3 (Ac-HH3), acetylated histone H4 (Ac-HH4), p21, and acetylated tubulin (Ac-tubulin) in U937 cells after a) 6 h and b) 24 h of treatment with compounds at 1 μM. Tubulin was used as a loading control.

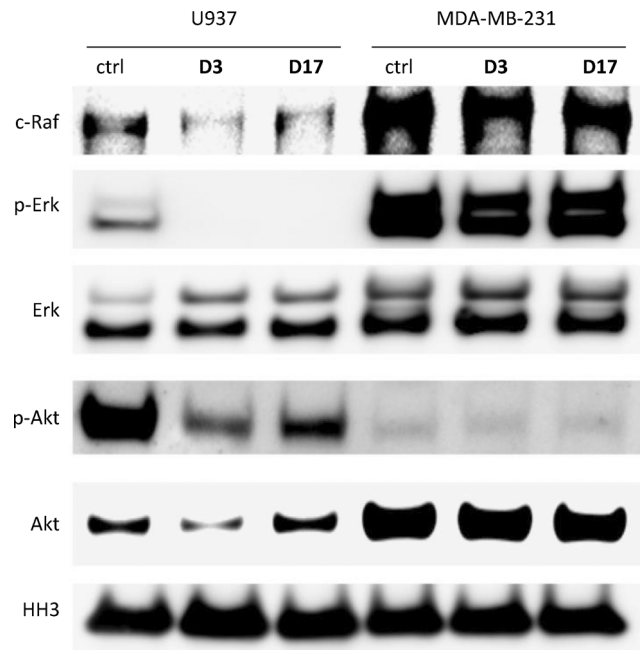

Figure 5. Western blot analysis of c-Raf, p-Erk, Erk, p-Akt, Akt and histone H3 (HH3) in U937 and MDA-MB-231 cell line after 24 h of treatment with **D3** and **D17** at 1 μM. Histone H3 was used as a loading control.

ecules cannot lower the signal. However, the tested molecules can clearly decrease the levels of c-Raf and p-Erk proteins without decreasing the expression of Erk protein in U937 cells. Regarding the PI3K/AKT/mTOR cell proliferation pathway, although MDA-MB-231 cells have high levels of Akt protein, p-Akt levels are very low, indicating that MDA-MB-231 cells do not depended on the PI3K/AKT/mTOR signaling pathway for growth and survival. In contrast, although U937 cells have lower Akt levels, p-Akt levels are very high, which can be significantly decreased by compounds **D3** and **D17**. Based on our results, we can attribute the sensitivity of U937 cells toward the tested inhibitors to their effects on these two oncogenic pathways, which are critical for cancer cell survival. To the best of our knowledge, the work presented herein constitutes the first report of a mechanistic difference in the antitumor activity of HDAC inhibitors between non-solid (U937) and solid (MDA-MB-231) tumor cell lines. Further detailed mechanistic studies are being carried out to support these findings, and will be reported in due course.

Conclusions

A series of HDAC inhibitors was synthesized by structural modification of a lead compound and evaluated by enzyme inhibition assays, in vitro and in vivo antiproliferation assays, isoform selectivity tests, and western blot analysis. Significant improvements in enzyme inhibitory activity were observed by changing the Boc group to substituted aromatic groups. The MTT assays show that the derived molecules are potent antiproliferative agents, particularly against non-solid tumor cell lines such as U937, K562, and HL60. In the in vivo antitumor assays using athymic nude mice inoculated with U937 cells, compound **D17** shows better performance than the positive control, SAHA. The evidence highlights the value of **D17** for further development. Isoform selectivity studies show that the representative compounds are generally more prone to bind to class I HDACs (HDAC1, HDAC2, and HDAC3) than HDAC6. Western blot assays revealed that the representative molecules can block the action of both class I HDACs and HDAC6. The difference in antitumor mechanism between non-solid (U937) and solid tumor cells (MDA-MB-231) was investigated by western blot analysis. The MAPK and PI3K/AKT/mTOR signaling pathways were found to render U937 cells rather than MDA-MD-231 cells sensitive to the tested molecules.

Experimental Section

General: All commercially available starting materials, reagents, and solvents were used without further purification. All reactions were monitored by TLC with 0.25 mm silica gel plates ($60\,GF_{254}$); UV light and $FeCl_3$ were used to visualize the spots. ^1H NMR spectra were recorded on a Bruker DRX spectrometer at 600 MHz, using TMS as an internal standard. High-resolution mass spectra were performed at the Shandong Analysis and Test Center in Ji'nan, China. Melting points were determined on an Electrothermal melting point apparatus and are uncorrected. Optical rotation values were measured at room temperature using a modular circular polarimeter 200 operating at $\lambda = 589$ nm. Maximum absorption wavelengths of the target compounds were detected for HPLC analysis. The compounds were dissolved in MeOH at a concentration of 1 mg per 100 mL and scanned from 500 to 200 nm using a UV-2102PCS spectrophotometer. All the derived target compounds are $>95\%$ pure, as determined by HPLC analysis, performed on an Agilent 1100 HPLC instrument using a Phenomenex Synergi 4 μm Hydro-RP 80A column (250 mm × 4.6 mm). All the target compounds were eluted with CH_3CN and H_2O (containing 0.1% formic acid) at various proportions, detected at their maximum absorption wavelengths.

Supporting Information: ^1H and ^{13}C NMR spectra, HPLC traces, and HRMS spectra for final compounds **D1**–**D19** are given in the Supporting Information.

(*S*)-Methyl 4-(2-((*tert*-butoxycarbonyl)amino)-2-phenylacetamido)benzoate (a): This compound was synthesized as described in our previous work.[8b]

(*S*)-Methyl 4-(2-amino-2-phenylacetamido)benzoate hydrochloride (b): To a solution of **e** (3.84 g, 10 mmol) in EtOAc (30 mL), a solution of EtOAc (30 mL) saturated with dry HCl gas was added. The reaction was stirred at RT for 5 h. The resultant precipitate was isolated by filtration, rinsed with Et_2O, and dried to give desired compound **b** (2.18 g, 68%): MS (ESI): *m/z* (%): 285.3 $[M+H]^+$; HRMS (AP-ESI) *m/z* calcd for $C_{15}H_{16}N_3O_3$ $[M+H]^+$ 286.1191, found 286.1186.

Preparation of c1 and its analogues: Derivatives **c2**–**c17** were prepared as described for **c1** (see below).

(*S*)-Methyl 4-(2-(4-chlorobenzamido)-2-phenylacetamido)benzoate (c1): To a solution of **b** (0.96 g, 3.0 mmol) in THF (50 mL)/H_2O (1.0 mL), $NaHCO_3$ (1.01 g, 12 mmol) was added. After 10 min, 4-chlorobenzoyl chloride (0.58 g, 3.3 mmol) was added. The reaction solution was stirred at RT for 8 h. Then, the solvent was evaporated, and the residue was taken up in EtOAc (50 mL). The EtOAc solution was washed with saturated aq citric acid (3 × 20 mL), saturat-

ed aq $NaHCO_3$ (3×20 mL), and brine (3×20 mL), dried over $MgSO_4$, and concentrated in vacuo. Desired compound **c1** was obtained by crystallization from EtOAc as a white powder (0.89 g, 70%): ^{1}H NMR (600 MHz, [D$_6$]DMSO): δ=10.76 (s, 1H), 9.20 (d, J=6.6 Hz, 1H), 7.97 (d, J=7.8 Hz, 2H), 7.92 (d, J=8.4 Hz, 2H), 7.76 (d, J=8.4 Hz, 2H), 7.58 (d, J=7.2 Hz, 2H), 7.54 (d, J=8.4 Hz, 2H), 7.42–7.39 (m, 2H), 7.36–7.34 (m, 1H), 5.83 (d, J=7.2 Hz, 1H), 3.82 ppm (s, 3H).

(*S*)-Methyl 4-(2-(2-chlorobenzamido)-2-phenylacetamido)benzoate (c2): White powder (0.91 g, 74%): ^{1}H NMR (600 MHz, [D$_6$]DMSO): δ=10.80 (s, 1H), 9.34 (d, J=7.2 Hz, 1H), 7.93 (d, J=7.8 Hz, 2H), 7.76 (d, J=7.8 Hz, 2H), 7. 58 (d, J=7.8 Hz, 2H), 7.50–7.44 (m, 3H), 7.40–7.38 (m, 3H), 7.35–7.32 (m, 1H), 5.85 (d, J=7.2 Hz, 1H), 3.82 ppm (s, 3H).

(*S*)-Methyl 4-(2-(2-naphthamido)-2-phenylacetamido)benzoate (c3): White powder (0.98 g, 77%): ^{1}H NMR (600 MHz, [D$_6$]DMSO): δ=10.79 (s, 1H), 9.23 (d, J=7.2 Hz, 1H), 8.61 (s, 1H), 8.04 (d, J=7.8 Hz, 1H), 8.02–7.98 (m, 3H), 7.93 (d, J=9.0 Hz, 2H), 7.78 (d, J=8.4 Hz, 2H), 7.64–7.59 (m, 4H), 7.44–7.41 (m, 2H), 7.36 (t, J=7.2 Hz, 1H), 5.91 (d, J=7.2 Hz, 1H), 3.82 ppm (s, 3H).

(*S*)-Methyl 4-(2-(4-fluorobenzamido)-2-phenylacetamido)benzoate (c4): White powder (0.88 g, 75%): ^{1}H NMR (600 MHz, [D$_6$]DMSO): δ=10.72 (s, 1H), 9.12 (d, J=7.2 Hz, 1H), 8.03–8.01 (m, 2H), 7.92 (d, J=9.0 Hz, 2H), 7.75 (d, J=9.0 Hz, 2H), 7.57 (d, J=7.8 Hz, 2H), 7.42–7.39 (m, 2H), 7.36–7.33 (m, 1H), 7.31–7.28 (m, 2H), 5.82 (d, J=7.2 Hz, 1H), 3.82 ppm (s, 3H).

(*S*)-Methyl 4-(2-(naphthalene-1-sulfonamido)-2-phenylacetamido)benzoate (c5): White powder (1.09 g, 79%): ^{1}H NMR (600 MHz, [D$_6$]DMSO): δ=10.47 (s, 1H), 9.15 (d, J=9.6 Hz, 1H), 8.73 (d, J=8.4 Hz, 1H), 8.13 (d, J=7.2 Hz, 1H), 8.06 (d, J=8.4 Hz, 1H), 7.95 (d, J=8.4 Hz, 1H), 7.83 (d, J=9.0 Hz, 2H), 7.67–7.65 (m, 1H), 7.61–7.58 (m, 1H), 7.53–7.50 (m, 1H), 7.41 (d, J=8.4 Hz, 2H), 7.29–7.28 (m, 2H), 7.17–7.16 (m, 3H), 5.20 (d, J=9.6 Hz, 1H), 3.81 ppm (s, 3H).

(*S*)-Methyl 4-(2-(4-(*tert*-butyl)phenylsulfonamido)-2-phenylacetamido)benzoate (c6): White powder (1.03 g, 74%): ^{1}H NMR (600 MHz, [D$_6$]DMSO): δ=10.52 (s, 1H), 8.73 (d, J=9.6 Hz, 1H), 7.84 (d, J=8.4 Hz, 2H), 7.66 (d, J=7.8 Hz, 2H), 7.50 (d, J=8.4 Hz, 2H), 7.37–7.36 (m, 4H), 7.27–7.23 (m, 3H), 5.17 (d, J=9.6 Hz, 1H), 3.80 (s, 3H), 1.17 ppm (s, 9H).

(*S*)-Methyl 4-(2-benzamido-2-phenylacetamido)benzoate (c7): White powder (1.07 g, 72%): ^{1}H NMR (600 MHz, [D$_6$]DMSO): δ=10.72 (s, 1H), 9.07 (d, J=7.2 Hz, 1H), 7.94 (d, J=9.0 Hz, 2H), 7.92 (d, J=9.0 Hz, 2H), 7.75 (d, J=9.0 Hz, 2H), 7.58 (d, J=7.8 Hz, 2H), 7.56–7.54 (m, 1H), 7.47 (t, J=7.8 Hz, 2H), 7.42–7.39 (m, 2H), 7.36–7.33 (m, 1H), 5.84 (d, J=7.2 Hz, 1H), 3.82 ppm (s, 3H).

(*S*)-Methyl 4-(2-phenyl-2-(4-(trifluoromethyl)phenylsulfonamido)acetamido)benzoate (c8): White powder (1.08 g, 75%): ^{1}H NMR (600 MHz, [D$_6$]DMSO): δ=10.61 (s, 1H), 9.14 (d, J=9.6 Hz, 1H), 7.91 (d, J=8.4 Hz, 2H), 7.85 (d, J=9.0 Hz, 2H), 7.75 (d, J=8.4 Hz, 2H), 7.48 (d, J=8.4 Hz, 2H), 7.36 (d, J=7.2 Hz, 2H), 7.26–7.22 (m, 3H), 5.24 (d, J=9.6 Hz, 1H), 3.81 ppm (s, 3H).

(*S*)-Methyl 4-(2-(2,6-difluorophenylsulfonamido)-2-phenylacetamido)benzoate (c9): White powder (1.02 g, 76%): ^{1}H NMR (600 MHz, [D$_6$]DMSO): δ=10.66 (s, 1H), 9.37 (d, J=9.6 Hz, 1H), 7.88 (d, J=9.0 Hz, 2H), 7.57 (d, J=9.0 Hz, 2H), 7.55–7.53 (m, 1H), 7.46 (d, J=9.0 Hz, 2H), 7.31–7.29 (m, 2H), 7.26 (t, J=7.2 Hz, 1H), 7.11 (t, J=9.0 Hz, 2H), 5.38 (d, J=9.6 Hz, 1H), 3.81 ppm (s, 3H).

(*S*)-Methyl 4-(2-(4-chlorophenylsulfonamido)-2-phenylacetamido)benzoate (c10): White powder (1.02 g, 77%): ^{1}H NMR (600 MHz, [D$_6$]DMSO): δ=10.59 (s, 1H), 8.97 (d, J=9.6 Hz, 1H), 7.88 (d, J=8.4 Hz, 2H), 7.71 (d, J=8.4 Hz, 2H), 7.52 (d, J=8.4 Hz, 2H), 7.46 (d, J=8.4 Hz, 2H), 7.37 (d, J=6.6 Hz, 2H), 7.29–7.25 (m, 3H), 5.20 (d, J=9.6 Hz, 1H), 3.81 ppm (s, 3H).

(*S*)-Methyl 4-(2-(2-methoxybenzamido)-2-phenylacetamido)benzoate (c11): White powder (0.95 g, 78%): ^{1}H NMR (600 MHz, [D$_6$]DMSO): δ=10.83 (s, 1H), 9.18 (d, J=7.2 Hz, 1H), 7.93 (d, J=8.4 Hz, 2H), 7.74 (d, J=8.4 Hz, 2H), 7.56 (d, J=7.8 Hz, 2H), 7.54 (d, J=8.4 Hz, 1H), 7.41 (t, J=7.8 Hz, 2H), 7.33 (t, J=7.2 Hz, 1H), 7.24 (d, J=9.0 Hz, 1H), 7.08 (t, J=7.2 Hz, 1H), 5.87 (d, J=7.2 Hz, 1H), 4.00 (s, 3H), 3.82 ppm (s, 3H).

(*S*)-Methyl 4-(2-(4-methoxybenzamido)-2-phenylacetamido)benzoate (c12): White powder (0.99 g, 82%): ^{1}H NMR (600 MHz, [D$_6$]DMSO): δ=10.70 (s, 1H), 8.89 (d, J=7.2 Hz, 1H), 7.94 (d, J=9.0 Hz, 2H), 7.92 (d, J=7.8 Hz, 2H), 7.75 (d, J=7.2 Hz, 2H), 7.57 (d, J=7.2 Hz, 2H), 7.40 (t, J=7.8 Hz, 2H), 7.34 (t, J=7.8 Hz, 1H), 6.99 (d, J=8.4 Hz, 2H), 5.82 (d, J=7.2 Hz, 1H), 4.02 (s, 3H), 3.81 ppm (s, 3H).

(*S*)-Methyl 4-(2-(3-bromobenzamido)-2-phenylacetamido)benzoate (c13): White powder (1.03 g, 76%): ^{1}H NMR (600 MHz, [D$_6$]DMSO): δ=10.72 (s, 1H), 9.27 (d, J=6.6 Hz, 1H), 8.16 (s, 1H), 7.93–7.91 (m, 3H), 7.76–7.74 (m, 3H), 7.57 (d, J=7.2 Hz, 2H), 7.45–7.40 (m, 3H), 7.35 (t, J=7.2 Hz, 1H), 5.81 (d, J=6.6 Hz, 1H), 3.82 ppm (s, 3H).

(*S*)-Methyl 4-(2-phenyl-2-(2-propylpentanamido)acetamido)benzoate (c14): White powder (0.91 g, 77%): ^{1}H NMR (600 MHz, [D$_6$]DMSO): δ=10.66 (s, 1H), 8.65 (d, J=7.2 Hz, 1H), 7.91 (d, J=8.4 Hz, 2H), 7.72 (d, J=8.4 Hz, 2H), 7.48 (d, J=7.8 Hz, 2H), 7.40–7.37 (m, 2H), 7.33–7.31 (m, 1H), 5.65 (d, J=7.2 Hz, 1H), 3.81 (s, 3H), 1.45–1.40 (m, 2H), 1.28–1.21 (m, 4H), 1.19–1.13 (m, 2H), 0.85 (m, 3H), 0.80 ppm (t, J=7.8 Hz, 3H).

(*S*)-Methyl 4-(2-phenyl-2-(2-phenylacetamido)acetamido)benzoate (c15): White powder (0.85 g, 73%): ^{1}H NMR (600 MHz, [D$_6$]DMSO): δ=10.77 (s, 1H), 9.02 (d, J=7.8 Hz, 1H), 7.90 (d, J=9.0 Hz, 2H), 7.72 (d, J=9.0 Hz, 2H), 7.50 (d, J=7.8 Hz, 2H), 7.40–7.37 (m, 2H), 7.33–7.31 (m, 1H), 7.30–7.28 (m, 4H), 7.22–7.19 (m, 1H), 5.63 (d, J=7.8 Hz, 1H), 3.81 (s, 3H), 3.59 ppm (m, 2H).

(*S*)-Methyl 4-(2-(naphthalene-2-sulfonamido)-2-phenylacetamido)benzoate (c16): White powder (1.08 g, 78%): ^{1}H NMR (600 MHz, [D$_6$]DMSO): δ=10.55 (s, 1H), 8.94 (d, J=9.6 Hz, 1H), 8.34 (s, 1H), 7.96–7.94 (m, 2H), 7.90 (d, J=8.4 Hz, 1H), 7.79–7.77 (m, 1H), 7.74 (d, J=9.0 Hz, 2H), 7.61–7.59 (m, 1H), 7.56–7.53 (m, 1H), 7.39–7.36 (m, 4H), 7.23 (t, J=7.2 Hz, 2H), 7.19–7.17 (m, 1H), 5.25 (d, J=8.4 Hz, 1H), 3.80 ppm (s, 3H).

(*S*)-Methyl 4-(2-(5-(dimethylamino)naphthalene-1-sulfonamido)-2-phenylacetamido)benzoate (c17): White powder (1.13 g, 75%): ^{1}H NMR (600 MHz, [D$_6$]DMSO): δ=10.40 (s, 1H), 9.06 (d, J=9.6 Hz, 1H), 8.37 (d, J=8.4 Hz, 1H), 8.28 (d, J=7.8 Hz, 1H), 8.12 (d, J=7.2 Hz, 1H), 7.81 (d, J=8.4 Hz, 2H), 7.55–7.52 (m, 1H), 7.49 (t, J=7.8 Hz, 1H), 7.40 (d, J=8.4 Hz, 2H), 7.30–7.29 (m, 2H), 7.18–7.16 (m, 4H), 5.17 (d, J=9.6 Hz, 1H), 3.80 (s, 3H), 2.71 ppm (s, 6H).

(*S*)-Methyl 4-(2-(3-(2-methoxyphenyl)ureido)-2-phenylacetamido)benzoate (c18): To a solution of triphosgene (1.5 g, 5.0 mmol) in dioxane (40 mL), 2-methoxyaniline (1.23 g, 10 mmol) was added. The reaction solution was stirred at 110 °C for 8 h. The solvent was evaporated to give a crude residue, which was sufficiently pure for use without further purification. The residue was redissolved in CH_2Cl_2 (50 mL), and **b** (1.6 g, 5.0 mmol) and Et_3N (0.61 g, 6.0 mmol) were added. The reaction was stirred at RT for 5 h. Then concentrated, and the residue was taken up in EtOAc (50 mL). The EtOAc

solution was washed with saturated aq citric acid (3×20 mL), saturated aq $NaHCO_3$ (3×20 mL), and brine (3×20 mL), dried over $MgSO_4$, and concentrated in vacuo. Desired compound **c18** was obtained by crystallization from EtOAc as a white powder (0.97 g, 45%); ^{1}H NMR (600 MHz, [D$_6$]DMSO): δ = 10.75 (s, 1H), 8.39 (s, 1H), 8.05 (d, J = 6.6 Hz, 1H), 7.91 (d, J = 8.4 Hz, 2H), 7.89 (d, J = 7.8 Hz, 1H), 7.74 (d, J = 8.4 Hz, 2H), 7.52 (d, J = 7.2 Hz, 2H), 7.42–7.39 (m, 2H), 7.34–7.32 (m, 1H), 6.97 (d, J = 7.8 Hz, 1H), 6.89–6.87 (m, 1H), 6.82 (t, J = 7.8 Hz, 1H), 5.56 (d, J = 7.8 Hz, 1H), 4.02 (s, 3H), 3.81 ppm (s, 3H).

(*S*)-Methyl 4-(2-(3-(2,6-diisopropylphenyl)ureido)-2-phenylacetamido)benzoate (c19): Prepared as described for **c18** (see above). White powder (0.61 g, 43%): ^{1}H NMR (600 MHz, [D$_6$]DMSO): δ = 10.76 (s, 1H), 7.92 (d, J = 8.4 Hz, 2H), 7.74 (s, 2H), 7.52 (d, J = 6.6 Hz, 2H), 7.40 (t, J = 6.6 Hz, 2H), 7.33–7.31 (m, 1H), 7.17 (d, J = 7.8 Hz, 2H), 7.10–7.18 (m, 2H), 5.59 (d, J = 8.4 Hz, 1H), 3.82 (s, 3H), 3.33 (s, 2H), 1.10 ppm (d, J = 6.6 Hz, 12H).

Preparation of D1–D19: Derivatives **D2**–**D19** were prepared as described for **D1** (see below).

(*S*)-4-Chloro-*N*-(2-((4-(hydroxycarbamoyl)phenyl)amino)-2-oxo-1-phenylethyl)benzamide (D1): Compound **g1** (0.5 g, 1.18 mmol) was dissolved in a solution of NH_2OK (0.56 g, 24 mmol) in methanol (14 mL). After 2 h at RT, the solvent was removed in vacuo. The residue was acidified to pH 3–4 with saturated aq citric acid solution, and the solution was extracted with EtOAc (3×20 mL). The organic layers were combined, washed with brine (3×20 mL) and dried over $MgSO_4$. Desired compound **D1** was obtained by crystallization from EtOAc as white powder (0.23 g, 54%): mp: 250–252 °C; $[\alpha]_D^{20} = -6.88$ (c = 1.0, MeOH); ^{1}H NMR (600 MHz, [D$_6$]DMSO): δ = 11.10 (s, 1H), 10.58 (s, 1H), 9.15 (d, J = 7.8 Hz, 1H), 8.93 (s, 1H), 7.98 (d, J = 8.4 Hz, 2H), 7.72 (d, J = 8.4 Hz,), 7.67 (d, J = 9.0 Hz,), 7.58 (d J = 7.2 Hz, 2H), 7.55 (d, J = 7.2 Hz, 1H), 7.42–7.39 (m, 2H), 7.36–7.34 (m, 1H), 5.84 ppm (d, J = 7.8 Hz, 1H); ^{13}C NMR (75 MHz, [D$_6$]DMSO): δ = 58.56, 118.96, 127.96, 128.18, 128.34, 128.59, 128.60, 129.03, 132.88, 136.76, 137.60, 141.77, 164.26, 166.04, 169.51 ppm; HRMS (AP-ESI): m/z $[M+H]^+$ calcd for $C_{22}H_{19}ClN_3O_4$: 424.1064, found: 424.1057; HPLC (λ = 266 nm): t_R = 9.6 min (CH_3CN/H_2O, 45:55).

(*S*)-2-Chloro-*N*-(2-((4-(hydroxycarbamoyl)phenyl)amino)-2-oxo-1-phenylethyl)benzamide (D2): Crystallized from EtOAc to give a white powder (0.22 g, 45%): mp: 250–252 °C; $[\alpha]_D^{20} = -8.20$ (c = 1.0, MeOH); ^{1}H NMR (600 MHz, [D$_6$]DMSO): δ = 11.11 (s, 1H), 10.62 (s, 1H), 9.29 (d, J = 7.8 Hz, 1H), 8.93 (s, 1H), 7.73 (d, J = 9 Hz, 2H), 7.67 (d, J = 8.4 Hz, 2H), 7.58 (d, J = 7.8 Hz, 2H), 7.48 (d, J = 6.6 Hz, 1H), 7.47 (d, J = 4.8 Hz, 1H), 7.45 (d, J = 8.4 Hz, 1H), 7.41–7.40 (m, 2H), 7.38 (t, J = 8.4 Hz, 1H), 7.35–7.32 (m, 1H), 5.86 ppm (d, J = 7.8 Hz, 1H); ^{13}C NMR (75 MHz, [D$_6$]DMSO): δ = 58.06, 118.97, 127.35, 127.97, 128.25, 128.46, 128.97, 129.76, 129.93, 131.34, 136.55, 137.70, 141.71, 164.24, 166.78, 169.20 ppm; HRMS (AP-ESI): m/z $[M+H]^+$ calcd for $C_{22}H_{19}ClN_3O_4$: 424.1064, found: 424.1057; HPLC (λ = 274 nm): t_R = 7.5 min (CH_3CN/H_2O, 40:60).

(*S*)-*N*-(2-((4-(Hydroxycarbamoyl)phenyl)amino)-2-oxo-1-phenylethyl)-2-naphthamide (D3): Crystallized from EtOAc to give a white powder (0.24 g, 47%): mp: 238–240 °C; $[\alpha]_D^{20} = -7.01$ (c = 1.0, MeOH); ^{1}H NMR (600 MHz, [D$_6$]DMSO): δ = 11.13 (s, 1H), 10.77 (s, 1H), 9.22 (d, J = 7.2 Hz, 1H), 8.93 (s, 1H), 8.63 (s, 1H), 8.05 (d, J = 7.8 Hz, 1H), 8.03 (d, J = 9.0 Hz, 1H), 8.02 (d, J = 8.4 Hz, 1H), 8.00 (d, J = 9.0 Hz, 1H), 7.74–7.71 (m, 2H), 7.65 (d, J = 7.8 Hz, 2H), 7.63–7.62 (m, 1H), 7.62–7.60 (m, 1H), 7.44–7.41 (m, 2H), 7.37–7.35 (m, 1H), 5.95 ppm (d, J = 7.8 Hz, 1H); ^{13}C NMR (75 MHz, [D$_6$]DMSO): δ = 58.66, 119.01, 125.07, 127.13, 127.92, 128.04, 128.16, 128.38, 128.40, 128.65, 128.70, 128.94, 129.36, 131.41, 132.50, 134.71, 137.96, 141.91, 164.25, 166.96, 169.69 ppm; HRMS (AP-ESI): m/z $[M+H]^+$ calcd for $C_{26}H_{22}N_3O_4$: 440.1610, found: 440.1607; HPLC (λ = 272 nm): t_R = 8.8 min (CH_3CN/H_2O, 45:55).

(*S*)-4-Fluoro-*N*-(2-((4-(hydroxycarbamoyl)phenyl)amino)-2-oxo-1-phenylethyl)benzamide (D4): Crystallized from EtOAc to give a white powder (0.22 g, 46%): mp: 240–242 °C; $[\alpha]_D^{20} = -5.64$ (c = 1.0, MeOH); ^{1}H NMR (600 MHz, [D$_6$]DMSO): δ = 11.12 (s, 1H), 10.65 (s, 1H), 9.10 (d, J = 7.2 Hz, 1H), 8.93 (s, 1H), 8.05–8.03 (m, 2H), 7.72 (d, J = 8.4, 2H), 7.69 (d, J = 9, 2H), 7.59 (d, J = 9.0 Hz, 2H), 7.42–7.39 (m, 2H), 7.35 (t, J = 7.2 Hz, 1H), 7.30 (t, J = 9.0 Hz, 1H), 5.86 ppm (d, J = 7.2 Hz, 1H); ^{13}C NMR (75 MHz, [D$_6$]DMSO): δ = 58.61, 115.58, 118.98, 127.90, 128.17, 128.43, 128.91, 130.60, 130.62, 137.79, 141.86, 163.66, 164.27, 165.93, 169.61 ppm; HRMS (AP-ESI): m/z $[M+H]^+$ calcd for $C_{22}H_{19}FN_3O_4$: 408.1359, found: 408.1355; HPLC (λ = 272 nm): t_R = 7.7 min (CH_3CN/H_2O, 40:60).

(*S*)-*N*-Hydroxy-4-(2-(naphthalene-1-sulfonamido)-2-phenylacetamido)benzamide (D5): Crystallized from EtOAc/hexane (1:1) to give a white powder (0.30 g, 53%): mp: 152–154 °C; $[\alpha]_D^{20} = -7.60$ (c = 1.0, MeOH); ^{1}H NMR (600 MHz, [D$_6$]DMSO): δ = 11.07 (s, 1H), 10.33 (s, 1H), 9.09 (d, J = 9 Hz, 1H), 8.92 (s, 1H), 8.74 (d, J = 8.4 Hz, 1H), 8.14–8.13 (m, 1H), 8.08 (d, J = 7.8 Hz, 1H), 7.96 (d, J = 8.4 Hz, 1H), 7.68–7.66 (m, 1H), 7.63 (d, J = 8.4 Hz, 1H), 7.60 (d, J = 7.8 Hz, 2H), 7.52 (t, J = 7.8 Hz, 2H), 7.34 (d, J = 9 Hz, 2H), 7.29 (d, J = 7.8 Hz, 1H), 7.18–7.16 (m, 1H), 5.21 ppm (d, J = 8.4 Hz, 1H); HRMS (AP-ESI): m/z $[M+H]^+$ calcd for $C_{25}H_{22}N_3O_5S$: 476.1280, found: 476.1273; HPLC (λ = 273 nm): t_R = 13.0 min (CH_3CN/H_2O, 40:60).

(*S*)-4-(2-(4-(*tert*-Butyl)phenylsulfonamido)-2-phenylacetamido)-*N*-hydroxybenzamide (D6): Crystallized from EtOAc/hexane (1:1) to give a white powder (0.27 g, 48%): mp: 155–157 °C; $[\alpha]_D^{20} = -7.77$ (c = 1.0, MeOH); ^{1}H NMR (600 MHz, [D$_6$]DMSO): δ = 11.08 (s, 1H), 10.39 (s, 1H), 8.93 (s, 1H), 8.67 (d, J = 9.6 Hz, 1H), 7.67 (d, J = 8.4 Hz, 2H), 7.66 (d, J = 8.4 Hz, 2H), 7.41 (d, J = 9 Hz, 2H), 7.39–7.27(m, 4H), 7.27 (d, J = 8.4 Hz, 2H), 7.25–7.23 (m, 1H), 5.17 (d, J = 10.2, 1H), 1.14 ppm (s, 9H); ^{13}C NMR (75 MHz, [D$_6$]DMSO): δ = 60.19, 118.99, 125.88, 126.96, 127.46, 128.01, 128.04, 128.26, 128.76, 137.24, 138.07, 141.19, 155.62, 164.07, 168.17 ppm; HRMS (AP-ESI): m/z $[M+H]^+$ calcd for $C_{25}H_{28}N_3O_5S$: 482.1749, found: 482.1743; HPLC (λ = 272 nm): t_R = 10.6 min (CH_3CN/H_2O, 45:55).

(*S*)-4-(2-Benzamido-2-phenylacetamido)-*N*-hydroxybenzamide (D7): Crystallized from EtOAc to give a white powder (0.19 g, 42%): mp: 229–230 °C; $[\alpha]_D^{20} = -6.60$ (c = 1.0, MeOH); ^{1}H NMR (600 MHz, [D$_6$]DMSO): δ = 11.10 (s, 1H), 10.59 (s, 1H), 9.02 (d, J = 7.8 Hz, 1H), 8.9 (s, 1H), 7.95 (d, J = 7.2 Hz, 2H), 7.72 (d, J = 9 Hz, 2H), 7.67 (d, J = 9 Hz, 2H), 7.59 (d, J = 7.8 Hz, 1H), 7.56 (t, J = 7.2 Hz, 2H), 7.48 (t, J = 7.8 Hz, 2H), 7.46–7.36 (m, 2H), 7.35 (t, J = 7.2 Hz, 1H), 5.86 ppm (d, J = 7.2 Hz, 1H); ^{13}C NMR (75 MHz, [D$_6$]DMSO): δ = 58.49, 118.95, 127.93, 128.17, 128.27, 128.34, 128.60, 128.93, 131.94, 134.13, 137.84, 141.82, 164.27, 166.97, 169.94 ppm; HRMS (AP-ESI): m/z $[M+H]^+$ calcd for $C_{22}H_{20}N_3O_4$: 390.1454, found: 390.1449; HPLC (λ = 270 nm): t_R = 9.9 min (CH_3CN/H_2O, 35:65).

(*S*)-*N*-Hydroxy-4-(2-phenyl-2-(4-(trifluoromethyl)phenylsulfonamido)acetamido)benzamide (D8): Crystallized from EtOAc/hexane (1:1) to give a white powder (0.23 g, 40%): mp: 200–202 °C; $[\alpha]_D^{20} = -7.20$ (c = 1.0, MeOH); ^{1}H NMR (600 MHz, [D$_6$]DMSO): δ = 11.10 (s, 1H), 10.48 (s, 1H), 9.09 (d, J = 9.6 Hz, 1H), 8.94 (s, 1H), 7.92 (d, J = 8.4 Hz, 2H), 7.76 (d, J = 8.4 Hz, 2H), 7.67 (d, J = 9 Hz, 2H), 7.41 (d, J = 8.4 Hz, 2H), 7.37 (d, J = 7.8 Hz, 2H), 7.26 (d, J = 8.4 Hz, 2H), 7.23–7.22 (m, 1H), 5.24 ppm (d, J = 9 Hz, 1H); ^{13}C NMR (75 MHz, [D$_6$]DMSO): δ = 60.18, 119.02, 127.52, 127.54, 127.99, 128.07, 128.79, 128.82, 128.86, 136.72, 140.99, 144.96, 164.08, 167.83 ppm; HRMS

(AP-ESI): *m/z* $[M+H]^+$ calcd for $C_{22}H_{19}F_3N_3O_5S$: 494.0997, found: 494.0993; HPLC ($\lambda=269$ nm): $t_R=8.6$ min (CH_3CN/H_2O, 45:55).

(*S*)-4-(2-(2,6-Difluorophenylsulfonamido)-2-phenylacetamido)-*N*-hydroxybenzamide (D9): Crystallized from EtOAc/hexane (1:1) to give a white powder (0.26 g, 47%): mp: 215–217 °C; $[\alpha]_D^{20}=-8.40$ ($c=1.0$, MeOH); ^{1}H NMR (600 MHz, [D$_6$]DMSO): $\delta=11.09$ (s, 1H), 10.52 (s, 1H), 9.29 (d, $J=9$ Hz, 2H), 8.93 (s, 1H), 7.68 (d, $J=9$ Hz, 2H), 7.56 (m, 1H), 7.49 (d, $J=8.4$ Hz, 2H), 7.46 (d, $J=7.8$ Hz, 2H), 7.32–7.9 (m, 2H), 7.27 (d, $J=7.2$ Hz, 1H), 7.12 (t, $J=9$ Hz, 2H), 5.37 ppm (d, $J=9.6$ Hz, 1H); ^{13}C NMR (75 MHz, [D$_6$]DMSO): $\delta=$ 60.70, 113.45, 113.60, 118.85, 127.60, 128.18, 128.53, 128.87, 135.62, 136.91, 141.25, 158.16, 159.87, 164.18, 167.92 ppm; HRMS (AP-ESI): *m/z* $[M+H]^+$ calcd for $C_{21}H_{18}F_2N_3O_5S$: 462.0935, found: 462.0931; HPLC ($\lambda=267$ nm): $t_R=8.3$ min (CH_3CN/H_2O, 40:60).

(*S*)-4-(2-(4-Chlorophenylsulfonamido)-2-phenylacetamido)-*N*-hydroxybenzamide (D10): Crystallized from EtOAc/hexane (1:1) to give a white powder (0.24 g, 45%): mp: 228–230 °C; $[\alpha]_D^{20}=-7.60$ ($c=1.0$, MeOH); ^{1}H NMR (600 MHz, [D$_6$]DMSO): $\delta=11.10$ (s, 1H), 10.46 (s, 1H), 8.93 (d, $J=7.2$ Hz, 1H), 8.92 (s, 1H), 7.72 (d, $J=$ 8.4 Hz, 2H), 7.68 (d, $J=9.0$ Hz, 2H), 7.47 (d, $J=7.2$ Hz, 2H), 7.44 (d, $J=8.4$ Hz, 2H), 7.38 (d, $J=7.8$ Hz, 2H), 7.28 (d, $J=8.4$ Hz, 2H), 7.26–7.25 (m, 1H), 5.20 ppm (d, $J=7.2$ Hz, 1H); ^{13}C NMR (75 MHz, [D$_6$]DMSO): $\delta=60.20$, 119.05, 128.21, 128.85, 128.98, 129.13, 129.25, 129.30, 136.97, 137.60, 140.03, 141.10, 164.14, 168.04 ppm; HRMS (AP-ESI): *m/z* $[M+H]^+$ calcd for $C_{21}H_{19}ClN_3O_5S$: 460.0734, found: 460.0725; HPLC ($\lambda=269$ nm): $t_R=10.3$ min (CH_3CN/H_2O, 40:60).

(*S*)-*N*-(2-((4-(Hydroxycarbamoyl)phenyl)amino)-2-oxo-1-phenylethyl)-2-methoxybenzamide (D11): Crystallized from EtOAc to give a white powder (0.23 g, 46%): mp: 156–158 °C; $[\alpha]_D^{20}=-7.50$ ($c=1.0$, MeOH); ^{1}H NMR (600 MHz, [D$_6$]DMSO): $\delta=11.11$ (s, 1H), 10.69 (s, 1H), 9.17 (d, $J=7.8$ Hz, 1H), 8.93 (s, 1H), 7.91 (d, $J=$ 7.8 Hz, 1H), 7.73 (d, $J=9$ Hz, 2H), 7.65 (d, $J=8.4$ Hz, 2H), 7.7–7.54 (m, 3H), 7.42–7.39 (m, 2H), 7.34 (d, $J=7.2$ Hz, 1H), 7.24 (d, $J=$ 8.4 Hz, 1H), 7.09 (t, $J=7.2$ Hz, 1H), 5.87 (d, $J=7.2$ Hz, 1H), 4.01 ppm (s, 3H); ^{13}C NMR (75 MHz, [D$_6$]DMSO): $\delta=56.83$, 17.75, 112.89, 119.15, 121.32, 121.37, 127.30, 128.27, 128.43, 129.18, 131.44, 133.67, 138.88, 141.43, 157.94, 164.08, 164.21, 169.28 ppm; HRMS (AP-ESI): *m/z* $[M+H]^+$ calcd for $C_{23}H_{22}N_3O_5$: 420.1559, found: 420.1553; HPLC ($\lambda=270$ nm): $t_R=8.2$ min (CH_3CN/H_2O, 40:60).

(*S*)-*N*-Hydroxy-4-(2-(4-methoxybenzamido)-2-phenylacetamido)-benzamide (D12): Crystallized from EtOAc to give a white powder (0.24 g, 49%): mp: 240–241 °C; $[\alpha]_D^{20}=-7.80$ ($c=1.0$, MeOH); ^{1}H NMR (600 MHz, [D$_6$]DMSO): $\delta=11.09$ (s, 1H), 10.55 (s, 1H), 8.91 (s, 1H), 8.83 (d, $J=7.8$ Hz, 1H), 7.95 (d, $J=7.2$ Hz, 2H), 7.72 (d, $J=$ 9.0 Hz, 2H), 7.67 (d, $J=9.0$ Hz, 2H), 7.57 (d, $J=7.2$ Hz, 2H), 7.41–7.39 (m, 2H), 7.35–7.33 (m, 2H), 7.00 (d, $J=8.4$ Hz, 2H), 5.84 (d, $J=$ 7.2 Hz, 1H), 3.82 ppm (s, 3H); ^{13}C NMR (75 MHz, [D$_6$]DMSO): $\delta=$ 55.73, 58.42, 113.81, 118.95, 126.31, 127.94, 128.21, 128.35, 128.92, 130.17, 137.96, 141.82, 162.24, 164.27, 166.42, 169.79 ppm; HRMS (AP-ESI): *m/z* $[M+H]^+$ calcd for $C_{23}H_{22}N_3O_5$: 420.1559, found: 420.1554; HPLC ($\lambda=265$ nm): $t_R=10.1$ min (CH_3CN/H_2O, 40:60).

(*S*)-3-Bromo-*N*-(2-((4-(hydroxycarbamoyl)phenyl)amino)-2-oxo-1-phenylethyl)benzamide (D13): Crystallized from EtOAc to give a white powder (0.26 g, 48%): mp: 234–236 °C; $[\alpha]_D^{20}=-6.80$ ($c=$ 1.0, MeOH); ^{1}H NMR (600 MHz, [D$_6$]DMSO): $\delta=11.10$ (s, 1H), 10.58 (s, 1H), 9.23 (d, $J=7.2$ Hz, 1H), 8.93 (s, 1H), 8.17 (s, 1H), 7.94 (d, $J=$ 7.8 Hz, 1H), 7.76 (d, $J=7.8$ Hz, 1H), 7.72 (d, $J=9.0$ Hz, 2H), 7.67 (d, $J=8.4$ Hz, 2H), 7.58 (d, $J=7.2$ Hz, 2H), 7.45 (d, $J=7.8$ Hz, 1H), 7.41 (d, $J=9.0$ Hz, 1H), 7.37–7.34 (m, 1H), 5.84 ppm (d, $J=7.8$ Hz, 1H); HRMS (AP-ESI): *m/z* $[M+H]^+$ calcd for $C_{22}H_{19}BrN_3O_4$: 468.0559, found: 468.0554; HPLC ($\lambda=270$ nm): $t_R=11.5$ min (CH_3CN/H_2O, 40:60).

(*S*)-*N*-Hydroxy-4-(2-phenyl-2-(2-propylpentanamido)acetamido)-benzamide (D14): Crystallized from EtOAc to give a white powder (0.23 g, 47%): mp: 267–269 °C; $[\alpha]_D^{20}=-7.20$ ($c=1.0$, MeOH); ^{1}H NMR (600 MHz, [D$_6$]DMSO): $\delta=11.09$ (s, 1H), 10.52 (s, 1H), 8.92 (s, 1H), 8.61 (d, $J=7.2$ Hz, 1H), 7.71 (d, $J=8.4$ Hz, 1H), 7.64 (d, $J=$ 8.4 Hz, 2H), 7.48 (d, $J=7.2$ Hz, 2H), 7.40–7.37 (m, 2H), 7.33–7.30 (m, 1H), 5.67 (d, $J=7.8$ Hz, 1H), 1.47–1.43 (m, 1H), 1.28–1.21 (m, 4H), 1.19–1.12 ppm (m, 6H); HRMS (AP-ESI): *m/z* $[M+H]^+$ calcd for $C_{23}H_{30}N_3O_4$: 412.2236, found: 412.2231; HPLC ($\lambda=271$ nm): $t_R=$ 11.9 min (CH_3CN/H_2O, 40:60).

(*S*)-*N*-Hydroxy-4-(2-phenyl-2-(2-phenylacetamido)acetamido)benzamide (D15): Crystallized from EtOAc to give a white powder (0.22 g, 46%): mp: 225–226 °C; $[\alpha]_D^{20}=-6.70$ ($c=1.0$, MeOH); ^{1}H NMR (600 MHz, [D$_6$]DMSO): $\delta=11.09$ (s, 1H), 10.56 (s, 1H), 8.92 (s, 1H), 8.91 (d, $J=8.4$ Hz, 1H), 7.71 (d, $J=9.0$ Hz, 2H), 7.63 (d, $J=$ 9.0 Hz, 2H), 7.50 (d, $J=7.2$ Hz, 2H), 7.40–7.37 (m, 2H), 7.33 (d, $J=$ 7.2 Hz, 1H), 7.29–7.28 (m, 4H), 7.22–7.20 (m, 1H), 5.65 (d, $J=$ 7.8 Hz, 1H), 3.60 ppm (s, 2H); ^{13}C NMR (75 MHz, [D$_6$]DMSO): $\delta=$ 42.10, 60.20, 118.96, 126.76, 128.22, 128.38, 129.00, 129.52, 136.77, 138.26, 141.68, 163.01, 169.59, 170.61 ppm; HRMS (AP-ESI): *m/z* $[M+H]^+$ calcd for $C_{23}H_{22}N_3O_4$: 404.1610, found: 404.1607; HPLC ($\lambda=269$ nm): $t_R=9.8$ min (CH_3CN/H_2O, 36:64).

(*S*)-*N*-Hydroxy-4-(2-(naphthalene-2-sulfonamido)-2-phenylacetamido)benzamide (D16): Crystallized from EtOAc/hexane (1:1) to give a white powder (0.30 g, 53%): mp: 196–198 °C; $[\alpha]_D^{20}=-6.90$ ($c=1.0$, MeOH); ^{1}H NMR (600 MHz, [D$_6$]DMSO): $\delta=11.07$ (s, 1H), 10.43 (s, 1H), 8.94 (s, 1H), 8.33 (s, 1H), 7.96 (d, $J=8.4$ Hz, 1H), 7.94 (d, $J=9.0$ Hz, 1H), 7.90 (d, $J=7.8$ Hz, 1H), 7.77 (d, $J=8.4$ Hz, 1H), 7.60 (t, $J=7.2$ Hz, 1H), 7.57 (s, 1H), 7.55 (d, $J=8.4$ Hz, 2H), 7.38 (d, $J=7.2$ Hz, 2H), 7.30 (d, $J=8.4$ Hz, 2H), 7.22 (t, $J=7.2$ Hz, 2H), 7.17 (d, $J=7.2$ Hz, 1H), 5.23 ppm (s, 1H); HRMS (AP-ESI): *m/z* $[M+H]^+$ calcd for $C_{25}H_{22}N_3O_5S$: 476.1280, found: 476.1276; HPLC ($\lambda=$ 271 nm): $t_R=9.6$ min (CH_3CN/H_2O, 43:57).

(*S*)-4-(2-(5-(Dimethylamino)naphthalene-1-sulfonamido)-2-phenylacetamido)-*N*-hydroxybenzamide (D17): Crystallized from EtOAc/hexane (1:1) to give a white powder (0.30 g, 49%): mp: 152–154 °C; $[\alpha]_D^{20}=-6.78$ ($c=1.0$, MeOH); ^{1}H NMR (600 MHz, [D$_6$]DMSO): $\delta=11.08$ (s, 1H), 10.28 (s, 1H), 9.04 (d, $J=9.6$ Hz, 1H), 8.94 (s, 1H), 8.37 (d, $J=8.4$ Hz, 1H), 8.29 (d, $J=8.4$ Hz, 1H), 8.12 (d, $J=7.2$ Hz, 1H), 7.60 (d, $J=9.0$ Hz, 2H), 7.55–7.53 (m, 1H), 7.51–7.48 (m, 1H), 7.31–7.29 (m, 4H), 7.18–7.16 (m, 4H), 5.16 (d, $J=9.6$ Hz, 1H), 2.71 ppm (s, 6H); HRMS (AP-ESI): *m/z* $[M+H]^+$ calcd for $C_{27}H_{27}N_4O_5S$: 519.1702, found: 519.1699; HPLC ($\lambda=262$ nm): $t_R=$ 10.2 min (CH_3CN/H_2O, 40:60).

(*S*)-*N*-Hydroxy-4-(2-(3-(2-methoxyphenyl)ureido)-2-phenylacetamido)benzamide (D18): Crystallized from EtOAc to give a white powder (0.17 g, 33%): mp: 201–203 °C; $[\alpha]_D^{20}=-6.40$ ($c=1.0$, MeOH); ^{1}H NMR (600 MHz, [D$_6$]DMSO): $\delta=11.09$ (s, 1H), 10.61 (s, 1H), 8.92 (s, 1H), 8.39 (s, 1H), 8.07 (s, 1H), 8.06 (d, $J=7.8$ Hz, 1H), 7.88 (d, $J=7.8$ Hz, 1H), 7.71 (d, $J=9.0$ Hz, 1H), 7.66 (d, $J=8.4$ Hz, 2H), 7.52 (d, $J=7.8$ Hz, 2H), 7.42–7.39 (m, 2H), 7.33 (t, $J=7.2$ Hz, 1H), 6.97 (d, $J=7.8$ Hz, 1H), 6.90–6.87 (m, 1H), 6.84–6.82 (m, 1H), 5.57 (d, $J=7.8$ Hz, 1H), 3.84 ppm (s, 3H); ^{13}C NMR (75 MHz, [D$_6$]DMSO): $\delta=57.98$, 60.19, 111.09, 118.47, 120.88, 121.63, 121.72, 127.11, 127.89, 129.02, 129.06, 129.62, 126.75, 139.06, 141.73, 147.90, 154.98, 164.27, 167.60 ppm; HRMS (AP-ESI): *m/z* $[M+H]^+$ calcd for $C_{23}H_{23}N_4O_5$: 435.1668, found: 435.1662; HPLC ($\lambda=$ 272 nm): $t_R=8.7$ min (CH_3CN/H_2O, 40:60).

(*S*)-4-(2-(3-(2,6-Diisopropylphenyl)ureido)-2-phenylacetamido)-*N*-hydroxybenzamide (D19): Crystallized from EtOAc to give a white powder (0.24 g, 42%): mp: 252–254 °C; $[\alpha]_D^{20} = -8.40$ ($c = 1.0$, MeOH); ^{1}H NMR (600 MHz, [D$_6$]DMSO): $\delta = 11.12$ (s, 1H), 10.67 (s, 1H), 8.95 (s, 1H), 7.77 (s, 1H), 7.71 (d, $J = 8.4$ Hz, 2H), 7.66 (d, $J = 7.8$ Hz, 2H), 7.52 (d, $J = 7.8$ Hz, 2H), 7.39 (d, $J = 7.2$ Hz, 2H), 7.32 (d, $J = 7.2$ Hz, 1H), 7.18 (s, 2H), 7.10 (s, 2H), 5.58 (d, $J = 8.4$ Hz, 1H), 3.16–3.13 (m, 2H), 1.11 ppm (d, $J = 7.2$ Hz, 12H); HRMS (AP-ESI): m/z $[M+H]^+$ calcd for $C_{28}H_{33}N_4O_4$: 489.2502, found: 489.2497; HPLC ($\lambda = 270$ nm): $t_R = 8.8$ min (CH_3CN/H_2O, 48:52).

Molecular docking studies

Docking was performed with Sybyl-X 2.0 and Maestro ver. 7.5 (Schrödinger Inc, supported by Shanghai Institute of Materia Medica Chinese Academy of Sciences). All the molecules sketched and minimized by Sybyl-X were ionized and assigned OPLS 2005 force field by LigPrep. The structure of human HDAC2, obtained from the RCSB Protein Data Bank (PDB entry: 3MAX) was used for the docking study. The HDAC2 structure was prepared by removal of waters and ligands, and assignment of OPLS 2005 force field using Maestro. The active site was defined as a cube of side length 20 Å, centered at the zinc ion by Glide dock. Extra precision was applied in the docking process; other parameters such as docking options, charges, core, constraints (zinc ion), and output ligand poses, were set as default.

Biological evaluations

In vitro HDAC inhibition assays: In vitro activity assay against HeLa cell nuclear extracts has been described in our previous work.[11] Briefly, HeLa cell nuclear extract solution (10 μL) was mixed with various concentrations of compound sample (50 μL). Fluorogenic substrate (40 μL) was added, and after 30 min incubation at 37 °C, the reaction was stopped by addition of developer (100 μL) containing trypsin and TSA. Fluorescence intensity was measured after 20 min of reaction using a microplate reader at respective excitation and emission wavelengths of 390 and 460 nm. The IC_{50} values were determined based on the fluorescence intensity readings. The procedures for HDAC1, 2, 3, and 6 assays were similar to that for HeLa nuclear extracts.

In vitro antiproliferative assays: Tumor cell inhibition was determined using the MTT method. Briefly, 2000 cells were seeded into each well of 96-well plates, which were incubated at 37 °C, 5% CO_2 overnight. The cells were then treated with compound sample at various concentrations for 48 h. Afterward, a 0.5% MTT solution was added to each well. After 4 h incubation, formazan formed from MTT was extracted by adding DMSO (200 μL) for 5 min. Optical density values were then detected at $\lambda = 570$ nm on a microplate reader.

In vivo antitumor assays against U937 xenografts: For in vivo antitumor efficacy studies, 1.8×10^7 U937 cells were inoculated subcutaneously in the right shoulder of male athymic nude mice (five to six weeks old, Slac Laboratory Animals, Shanghai, China). Ten days after injection, tumors were palpable, and mice were randomized into treatment and control groups (five mice per group). The treatment groups were administrated with 100 mg kg^{-1} d^{-1} intragastrically, the control group was administrated with an equal volume of PBS solution. During treatment, the body weight of mice was monitored regularly. After 16 days of administration, the mice were euthanized, and tumor weights were measured on an electronic balance. The experiments were approved by the Animal Experiment Ethical Review Board of Shandong University (approval No. 201302006).

Western blot analysis: For western blot analysis, total protein extracts were separated on a polyacrylamide gel, transferred onto PVDF membranes and blotted as previously described.[12] Briefly, U937 and MDA-MB-231 cells with different treatment were collected and lysed with lysis buffer for 30 min then centrifuged for 15 min at 4000 rpm at 4 °C; the supernatant contained the whole-cell extracts. Total protein extracts were separated by 12% SDS-PAGE and transferred onto PVDF membranes (Millipore, cat. no. IPVH00010). Membranes were blocked with 5% milk in TBS-T for 1 h at room temperature, then incubated with a 1:1000 or 1:2000 dilution of primary antibody overnight at 4 °C including tubulin (Sigma), acetylated tubulin (Sigma), histone H3 (Sigma), acetylated histone H3 (Sigma), acetylated histone H4 (Sigma), p21 (Cell Signaling), c-Raf (Sigma), p-Erk (Sigma), Erk (Sigma), p-Akt (Sigma), and Akt (Sigma). Membranes were then washed three times and incubated at a 1:2000 dilution of anti-mouse or anti-rabbit HRP-conjugated goat secondary antibodies for 2 h at room temperature. Finally, membranes were washed another three times and developed by enhanced chemiluminescence (ECL; Millipore, cat. no. WBKL S0050). Images were obtained using an Image Quant LAS 4000 imager. Complete gel images can be obtained from the Editorial Office or the authors upon request.

Acknowledgements

This work was supported by the National Nature Science Foundation of China (grant no. 21172134), the National High Technology Research & Development Program of China (grant no. 2011ZX09401-015), the Doctoral Foundation of the Ministry of Education of China (grant no. 20110131110037), the Independent Innovation Foundation of Shandong University (IIFSDU), China (grant no. 2013GN013) and the US National Cancer Institute (NCI), the US National Institutes of Health (NIH) (grant no. R01CA163452 to C.J.C.).

Keywords: antitumor agents · cancer · epigenetics · histone deacetylases · inhibitors · structural optimization

[1] a) B. E. Bernstein, J. K. Tong, S. L. Schreiber, *Proc. Natl. Acad. Sci. USA* **2000**, *97*, 13708–13713; b) A. J. M. De Ruijter, A. H. Van Gennip, H. N. Caron, S. Kemp, A. B. P. Van Kuilenburg, *Biochem. J.* **2003**, *370*, 737–749; c) C. Foglietti, G. Filocamo, E. Cundari, E. De Rinaldis, A. Lahm, R. Cortese, C. Steinkuhler, *J. Biol. Chem.* **2006**, *281*, 17968–17976.

[2] a) E. Grönroos, U. Hellman, C. H. Heldin, J. Ericsson, *Mol. Cell* **2002**, *10*, 483–493; b) V. Giandomenico, M. Simonsson, E. Grönroos, J. Ericsson, *Mol. Cell. Biol.* **2003**, *23*, 2587–2599; c) Y. H. Jin, E. J. Jeon, Q. L. Li, Y. H. Lee, J. K. Choi, W. J. Kim, K. Y. Lee, S. C. Bae, *J. Biol. Chem.* **2004**, *279*, 29409–29417.

[3] a) A. M. Bode, Z. G. Dong, *Nat. Rev. Cancer* **2004**, *4*, 793–805; b) L. F. Chen, W. C. Greene, *Nat. Rev. Mol. Cell Biol.* **2004**, *5*, 392–401; c) J. J. Kovacs, P. J. M. Murphy, S. Gaillard, X. A. Zhao, J. T. Wu, C. V. Nicchitta, M. Yoshida, D. O. Toft, W. B. Pratt, T. P. Yao, *Mol. Cell* **2005**, *18*, 601–607.

[4] P. A. Marks, R. A. Rifkind, V. M. Richon, R. Breslow, T. Miller, W. K. Kelly, *Nat. Rev. Cancer* **2001**, *1*, 194–202.

[5] a) S. A. M. Thiagalingam, K.-H. Cheng, H. J. Lee, N. Mineva, A. Thiagalingam, J. F. Ponte, *Ann. N. Y. Acad. Sci.* **2003**, *983*, 84–100; b) P. A. Marks, V. M. Richon, R. A. Rifkind, *J. Natl. Cancer Inst.* **2000**, *92*, 1210–1216.

[6] V. M. Richon, S. Emiliani, E. Verdin, Y. Webb, R. Breslow, R. A. Rifkind, P. A. Marks, *Proc. Natl. Acad. Sci. USA* **1998**, *95*, 3003–3007.

[7] H. Ueda, H. Nakajima, Y. Hori, T. Fujita, M. Nishimura, T. Goto, M. Okuhara, *J. Antibiot.* **1994**, *47*, 301 – 310.
[8] a) L. Zhang, M. Y. Li, J. H. Feng, H. Fang, W. F. Xu, *Med. Chem. Res.* **2012**, *21*, 152 – 156; b) L. Zhang, X. Wang, X. Li, W. Xu, *J. Enzyme Inhib. Med. Chem.* **2013**, DOI: 10.3109/14756366.2013.780237.
[9] a) I. Verbrugge, R. W. Johnstone, M. Bots, *Epigenomics* **2011**, *3*, 547 – 565; b) B. E. Gryder, Q. H. Sodji, A. K. Oyelere, *Future Med. Chem.* **2012**, *4*, 505 – 524.
[10] a) G. Garcia-Manero, H. Yang, C. Bueso-Ramos, A. Ferrajoli, J. Cortes, W. G. Wierda, S. Faderl, C. Koller, G. Morris, G. Rosner, A. Loboda, V. R. Fantin, S. S. Randolph, J. S. Hardwick, J. F. Reilly, C. Chen, J. L. Ricker, J. P. Secrist, V. M. Richon, S. R. Frankel, H. M. Kantarjian, *Blood* **2008**, *111*, 1060 – 1066; b) J. Vansteenkiste, E. Van Cutsem, H. Dumez, C. Chen, J. L. Ricker, S. S. Randolph, P. Schoffski, *Invest. New Drugs* **2008**, *26*, 483 – 488; c) P. N. Munster, M. Lacevic, M. Schmitt, E. Bicaku, D. Marchion, A. Stephens, L. Sullivan, S. Minton, *J. Clin. Oncol.* **2008**, *26*, 3501 (meeting abstract); d) E. Galanis, K. A. Jaeckle, M. J. Maurer, J. M. Reid, M. M. Ames, J. S. Hardwick, J. F. Reilly, A. Loboda, M. Nebozhyn, V. R. Fantin, V. M. Richon, B. Scheithauer, C. Giannini, P. J. Flynn, D. F. Moore, Jr., J. Zwiebel, J. C. Buckner, *J. Clin. Oncol.* **2009**, *27*, 2052 – 2058; e) K. Hymes, R. Dummer, W. Sterry, M. Steinhoff, C. Assaf, H. Kerl, J. Ahern, S. Rizvi, J. L. Ricker, S. Whittaker, *J. Clin. Oncol.* **2008**, *26*, 8613 (meeting abstract); f) M. Duvic, E. A. Olsen, D. Breneman, T. R. Pacheco, S. Parker, E. C. Vonderheid, R. Abuav, J. L. Ricker, S. Rizvi, C. Chen, K. Boileau, A. Gunchenko, C. Sanz-Rodriguez, L. J. Geskin, *Clin. Lymphoma Myeloma* **2009**, *9*, 412 – 416; g) R. L. Piekarz, R. Robey, V. Sandor, S. Bakke, W. H. Wilson, L. Dahmoush, D. M. Kingma, M. L. Turner, R. Altemus, S. E. Bates, *Blood* **2001**, *98*, 2865 – 2868; h) W. M. Stadler, K. Margolin, S. Ferber, W. McCulloch, J. A. Thompson, *Clinical Genitourin. Cancer* **2006**, *5*, 57 – 60; i) D. S. Schrump, M. R. Fischette, D. M. Nguyen, M. Zhao, X. Li, T. F. Kunst, A. Hancox, J. A. Hong, G. A. Chen, E. Kruchin, J. J. Wright, D. R. Rosing, A. Sparreboom, W. D. Figg, S. M. Steinberg, *Clin. Cancer Res.* **2008**, *14*, 188 – 198; j) R. P. Whitehead, C. Rankin, P. M. G. Hoff, P. J. Gold, K. G. Billingsley, R. A. Chapman, L. Wong, J. H. Ward, J. L. Abbruzzese, C. D. Blanke, *Invest. New Drugs* **2009**, *27*, 469 – 475.
[11] Y. J. Zhang, J. H. Feng, C. X. Liu, L. Zhang, J. Jiao, H. Fang, L. Su, X. P. Zhang, J. Zhang, M. Y. Li, B. H. Wang, W. F. Xu, *Bioorg. Med. Chem.* **2010**, *18*, 1761 – 1772.
[12] J. Feng, H. Fang, X. Wang, Y. Jia, L. Zhang, J. Jiao, J. Zhang, L. Gu, W. Xu, *Cancer Biol. Ther.* **2011**, *11*, 477 – 489.

Received: July 5, 2013
Revised: October 13, 2013
Published online on November 12, 2013